Research Paper

Mg-protoporphyrin IX monomethyl ester cyclase from *Rhodobacter capsulatus*: Radical SAM-dependent synthesis of the isocyclic ring of bacteriochlorophylls

Milan Wiesselmann[1], Stefanie Hebecker[1], José M. Borrero-de Acuña[1], Manfred Nimtz[2], David Bollivar[3], Lothar Jänsch[2], Jürgen Moser[1] and Dieter Jahn[4]

[1]Institute of Microbiology, Technische Universität Braunschweig, Spielmannstraße 7, D-38106 Braunschweig, Germany
[2]Cellular Proteome Research, Helmholtz Centre for Infection Research, Inhoffenstraße 7, D-38124 Braunschweig, Germany
[3]Department of Biology, Illinois Wesleyan University, Bloomington, IL 61702-2900, USA
[4]Braunschweig Centre of Integrated Systems Biology, Technische Universität Braunschweig, Rebenring 56, D-38106 Braunschweig, Germany

Correspondence: Jürgen Moser (j.moser@tu-bs.de)

Keywords: *Rhodobacter capsulatus*, chlorophyll, BchE, radical SAM enzyme, Mg-protoporphyrin IX monomethyl ester cyclase

Abstract:

During bacteriochlorophyll *a* biosynthesis, the oxygen-independent conversion of Mg-protoporphyrin IX monomethyl ester (Mg-PME) to protochlorophyllide (Pchlide) is catalyzed by the anaerobic Mg-PME cyclase termed BchE. Bioinformatics analyses in combination with pigment studies of cobalamin-requiring *Rhodobacter capsulatus* mutants indicated an unusual radical S-adenosylmethionine (SAM) and cobalamin-dependent BchE catalysis. However, *in vitro* biosynthesis of the isocyclic ring moiety of bacteriochlorophyll using purified recombinant BchE has never been demonstrated. We established a spectroscopic *in vitro* activity assay which was subsequently validated by HPLC analyses and $H_2{}^{18}O$ isotope label transfer onto the carbonyl-group (C-13^1-oxo) of the isocyclic ring of Pchlide. The reaction product was further converted to chlorophyllide in the presence of light-dependent Pchlide reductase. BchE activity was stimulated by increasing concentrations of NADPH or SAM, and inhibited by S-adenosylhomocysteine. Subcellular fractionation experiments revealed that membrane localized BchE requires an additional, heat-sensitive cytosolic component for activity. BchE catalysis was not sustained in chimeric experiments when a cytosolic extract from *E. coli* was used as a substitute. Size-fractionation of the soluble *R. capsulatus* fraction indicated that enzymatic activity relies on a specific component with an estimated molecular mass between 3 and 10 kDa. A structure guided site-directed mutagenesis approach was performed on the basis of a three-dimensional homology model of BchE. A newly established *in vivo* complementation assay was used to investigate 24 BchE mutant proteins. Potential ligands of the [4Fe-4S] cluster (Cys^{204}, Cys^{208}, Cys^{211}), of SAM (Phe^{210}, Glu^{308} and Lys^{320}) and of the proposed cobalamin cofactor (Asp^{248}, Glu^{249}, Leu^{29}, Thr^{71}, Val^{97}) were identified.

Introduction

The fundamental pathways for the synthesis of chlorophyll *a* or bacteriochlorophyll *a* (BChl *a*) are well described in the literature [1], but the enzymatic formation of the isocyclic ring moiety of these pigments still remains an obstacle [2-4]. Chlorophylls and BChls substantially differ from other tetrapyrroles due to the presence of this additional ring system (Ring E, Figure 1). The dedicated part of BChl *a* biosynthesis starts with the insertion of Mg^{2+} into protoporphyrin IX (PPIX) by the magnesium chelatase enzyme complex (BchH, BchI, BchD) [5]. The resulting Mg-PPIX is subsequently methylated by the Mg-PPIX methyltransferase (BchM) that generates Mg-PPIX monomethylester (Mg-PME). This is the substrate of two mechanistically unrelated Mg-PME cyclases which enable for the synthesis of the isocyclic ring (Figure 1). In both cases, the substrate Mg-PME is oxidatively cyclized to protochlorophyllide (Pchlide), which presumably includes the `oxygenation` of the unreactive C-13^1 methylene to hydroxymethylene (formally a 2 e^- oxidation), subsequent ketone formation (second 2 e^- oxidation) followed by C-C bond linkage between C-13^2 and C-15 (third 2 e^- oxidation) (Figure 1). To date, the intriguing six electron reactions of the two different Mg-PME cyclases have not been resolved at the biochemical level. Different intermediates of the BChl *a* pathway act as a substrate of an 8-vinyl reductase [6]. This is indicated by a substituent R which stands for 8-vinyl or 8-ethyl in Figure 1 (details of nomenclature in the caption).

The oxygen-dependent Mg-PME cyclase termed AcsF

The AcsF protein is conserved in higher plants, algae, cyanobacteria and some purple proteobacteria [7-9]. Bioinformatics-based amino acid sequence analyses classified AcsF as a non-heme diiron monooxygenase [10]. A series of studies indicated that additional subunits might be required to form an active cyclase [8, 11-14]. Only recently, three distinct classes of AcsF enzymes were delineated: AcsF proteins requiring either BciE or Ycf54 as an additional subunit or AcsF proteins that do not require further components [8]. The AcsF protein from the purple bacterial phototroph *Rubrivivax gelatinosus* belongs to the latter class. The respective *acsF* gene was expressed in *E. coli* and *in vivo* cyclase activity was observed when the cell culture was fed with Mg-PME, which diffuses across the bacterial membrane. Based on this important experiment, the overall chlorophyll biosynthetic pathway was successfully reconstituted in *E. coli* [4]. Recent work with the barley homolog demonstrated *in vitro* reconstitution of the AcsF/Ycf54 system [15]. With respect to the ´oxygenase´ activity of AcsF, key experiments were performed almost 30 years ago. They used whole cell $^{18}O_2$ labelling to demonstrate that the 13^1-oxo group of chlorophylls and BChls arises from molecular oxygen [16, 17].

The oxygen-independent Mg-PME cyclase termed BchE

Synthesis of BChl *a* in many purple bacteria is regulated at the level of gene expression by oxygen tension and light. Microaerophilic or anaerobic growth conditions strongly enhance photopigment biosynthesis in *R. capsulatus* [18, 19]. In this context, BchE facilitates the synthesis of Pchlide in the

absence of molecular oxygen. Interestingly, the genome of *R. capsulatus* does not encode for the alternative Mg-PME cyclase AcsF. With respect to the catalysis of BchE, pioneering *in vivo* $H_2{}^{18}O$ labeling experiments revealed that the 13^1-oxo group derives from a water molecule [20]. A conserved CxxxCxxC sequence motif was proposed to ligate a redox-active, oxygen-sensitive [4Fe-4S] cluster [21]. Bioinformatics studies classified BchE as a member of the radical S-adenosylmethionine (SAM) superfamily [22]. These proteins use a [4Fe-4S] cluster for the reductive cleavage of SAM to initiate subsequent radical chemistry. In addition, a potential C-terminal cobalamin cofactor binding domain was identified [22, 23]. Pigment analyses of cobalamin-requiring *R. capsulatus* mutants (*bluE* and *bluB*) suggested that BchE catalysis is based on cobalamin as an additional cofactor [23]. The direct *in vitro* verification of the proposed cofactor requirement with purified components is still pending. However, the three-dimensional structure of a structurally related cobalamin-dependent radical SAM enzyme named OxsB has recently been described. OxsB (in the presence of OxsA) catalyzes the formation of the unique four-membered ring structure of the antiviral compound oxetanocin in a net two e^- oxidation reaction. OxsB shares a moderate amino acid sequence identity of ~19% with BchE. The OxsB structure revealed an N-terminal radical SAM domain followed by a C-terminal domain with a bound hydroxo-cobalamin. This cofactor was found to be essential for OxsB activity, however its mechanistic function needs to be further clarified [24]. In a recent review, different cobalamin-dependent radical SAM mechanisms for the non-oxygenating conversion performed by OxsB and for the catalysis of BchE have been discussed [3]. It is clear that the unprecedented 6 e^- oxidative cyclization reactions of AcsF and BchE broaden the mechanistic repertoire of non-heme diiron monooxygenases and of the radical SAM superfamily. With respect to BchE, cobalamin-dependent radical SAM chemistry has been well characterized for methyl transferase reactions. However, the H_2O-dependent `oxygenation` of a substrate in the presence of a cobalamin-cofactor has been never exemplified for a radical SAM enzyme so far.

Up to this point, the absence of a reliable *in vitro* activity assay was hampering the further investigation of the sophisticated BchE catalysis. *R. capsulatus* is an appropriate organism for the investigation of BchE catalysis as the genome of this purple bacterium does not encode for the alternative Mg-PME cyclase AcsF.

Here we present the robust production and purification of the BchE substrate Mg-PME as a basis for the development of a reliable *in vitro* BchE activity assay. The kinetics of the conversion of Mg-PME into Pchlide was followed spectroscopically. The *in vitro* `oxygenation´ of the substrate was demonstrated by mass spectroscopy using $H_2{}^{18}O$ as a tracer. The subcellular localization of BchE and the requirement for an additional cyclase component were shown. An extensive site-directed mutagenesis approach enabled the characterization of potential ligands for of the iron sulfur center and of residues which interact with the SAM and cobalamin cofactors of BchE.

Experimental procedures

Bioinformatic analyses

The BchE amino acid sequence was analyzed for the presence of a potential signal sequence and transmembrane helices using the SignalP-5.0 [25] and the TMHMM Server v. 2.0 [26]. Homologous BchE proteins were identified by BLAST analyses [27]. Multiple amino acid sequence alignments were generated by Jalview [28]. A tentative three-dimensional model of BchE was generated using the SWISS-MODEL server [29] with the solved crystal structure of OxsB [24] (PDB code: 5UL3) as a template. PyMOL was used for the structural superposition with the cobalamin-bound OxsB structure to identify amino acid residues potentially involved in the binding of cofactors [30].

Bacterial strains and growth conditions

R. capsulatus strains (see supplemental Table S1) were grown in RCV [31] or RCV 2/3 PY medium [32] in the dark at 30°C and agitation at 100 rpm (Multitron Pro, Infors HT, Bottmingen, Switzerland). Cells from several colonies of plate grown *R. capsulatus* were used to inoculate a single 5 ml overnight preculture. Main cultures of 400 ml RCV 2/3 PY (in 1 l conical flasks with a start OD_{660} of 0.05) were cultivated for 16 h. The employed solid medium was PY Agar. Mutant strains or complemented mutant strains were grown with 25 µg/l kanamycin or 1 µg/ml gentamycin. *E. coli* cells (Table S1) were grown in baffled flasks containing LB medium at 37°C and 200 rpm with appropriate antibiotics at concentrations of 25 µg/ml kanamycin or 100 µg/ml ampicillin.

Production and purification of the BchE substrate Mg-PME

The *R. capsulatus* strain DB575 (strain *bchE*$^-$) was used to produce the BchE substrate. The overall Mg-PME yield was improved as detailed before for the biological production of chlorophyllide [33]. *R. capsulatus* DB575 was cultivated for 24 h in RCV 2/3 PY supplemented with 0.2% (w/v) Tween 80. The culture supernatant was applied to a Sep-Pak® C18 Plus Short Cartridges (Waters, USA) and Mg-PME was eluted using a stepwise acetone/water gradient from 20 to 80% (v/v) acetone (10% increments, 10 ml). UV/visible absorption spectra of the eluates were recorded (V-650, Jasco, Tokyo, Japan), fractions with a 595 nm / 633 nm ratio > 3.5 were combined and subsequently dried in a stream of nitrogen. Mg-PME was dissolved in 100 µl DMSO, stored at -20°C and the product concentration was determined using an extinction coefficient of 18.5 mM^{-1} cm^{-1} at a wavelength of 552 nm [34].

Production and purification of Pchlide and chlorophyllide

Pchlide was isolated from the *bchL*-deficient *R. capsulatus* strain ZY5 as described in [35]. Briefly, cells were cultivated in the presence of polyurethane foam bungs, which served as an affinity matrix for the adsorption of the excreted Pchlide. The green-colored foam bungs were dried at room temperature and the pigment was extracted with 100% acetone. Further purification was performed on CM Sepharose Fast Flow using a stepwise acetone/methanol gradient. The concentrated product was dissolved in DMSO. Chlorophyllide was isolated from the *bchF*- and *bchZ*-deficient *R. capsulatus* strain CB1200 as detailed in [33]. Briefly, the green colored culture supernatant was added to a C18 cartridge and after a

single washing step the pigment was eluted in acetone. The solvent was evaporated and the deep green product was dissolved in DMSO. In both cases, mixtures of the respective 8-vinyl or 8-ethyl derivatives were obtained.

***In vitro* cyclase activity assay**

The absence of BChl *a* biosynthetic intermediates in organic extracts of *R. capsulatus* ZY6 (*bchH*¯) cells was confirmed by fluorescence spectroscopy (Spectrofluorometer FP-8500, Jasco, Tokyo, Japan) as described elsewhere [36]. For BchE *in vitro* activity testing, *R. capsulatus* ZY6 (*bchH*¯) cells were grown microaerophilically into late stationary phase (indicated by a red coloring of the culture). For this purpose ten 1l flasks containing 400 ml RCV 2/3PY medium were cultivated for 16 h to an OD_{578} of ~1 at 100 rpm agitation in the dark. All subsequent steps were performed in an anoxic workstation (COY Laboratory Products, Grass Lake, USA). Cells from a culture volume of 200 ml were sedimented, resuspended in 250 µl 100 mM HEPES, pH 7.5 and 200 µl samples were stored at -20°C in sealed screw caps (micro tube 2 ml, Sarstedt, Nümbrecht, Germany) previously filled with 100 mg lysing matrix B (MP Biomedicals, Santa Ana, CA, USA). Aliquots were thawed at room temperature and 140 µM Mg-PME, 2 mM SAM, 2 mM NADPH and 2 mM DTT were added for subsequent *in vitro* activity testing. Reproducible cells lysis and the generation of a cell-free extract was ensured by using a FastPrep®-24 homogenizer (MP Biomedicals; Santa Ana, CA, USA) at a speed of 4.5 m/s for 30 s at 4°C (four cycles). This standard assay was incubated for 1 h at 30°C and stopped by addition of 500 µl acetone, vigorously mixing for 1 min, followed by 15 min centrifugation at 12´000 x g. Four hundred fifty µl of the resulting supernatants were extracted with 200 µl hexane to eliminate carotenoids [34]. Three hundred µl of the lower phase (water/acetone) was subjected to fluorescence spectroscopy using a FP-8500 Spectrofluorimeter (Jasco, Tokyo, Japan) with λ_{ex} = 438 nm. Spectra were recorded from 550 nm to 700 nm ($\lambda_{em\ Mg\text{-}PME}$ = 595 nm [37], $\lambda_{em\ Pchlide}$ = 633 nm [35], $\lambda_{em\ chlorophyllide}$ = 670 nm [35]). Control experiments in the absence of Mg-PME, without the cellular *R. capsulatus* extract or experiments in the presence of a BchE-depleted cellular extract (prepared from *R. capsulatus* DB575, *bchE*¯ strain) were performed. The standard *in vitro* assay was also performed with varying concentrations of SAM and NADPH or after air exposure for 10 min. Alternatively, inhibition of BchE activity was analyzed in the presence of EDTA (20 mM), 2,2´-bipyridyl (2 mM), S-adenosylhomocysteine (SAH) or Triton X-100.

Recombinant production and purification of *Dinoroseobacter shibae* LPOR

The LPOR gene (Dshi_4160) was PCR-amplified from genomic DNA of *D. shibae* DFL 12 using primers 1 and 2 (Table S2). Plasmid pGEX-6P-1_LPOR was generated using the InFusion HD cloning system according to the manufacturer's instructions (Takara, Kusatsu, Japan). Plasmid-containing *E. coli* BL21 cells were cultured at 37°C with 200 rpm agitation to an OD_{578} = 0.5 (0.5 l culture volume). Production of the N-terminal glutathione S-transferase fusion protein was induced by the addition of 25 µM IPTG. Cells were further cultivated at 17°C for 17 h, harvested by centrifugation and resuspended in 10 ml 100 mM HEPES, pH 7.5 containing 150 mM NaCl and 10 mM $MgCl_2$. Cell lysis was performed

by a single passage through a French Press® (Thermo Fisher Scientific, Waltham, MA, USA) at 14´500 psi followed by centrifugation for 60 min at 110´000 x g and 4°C. The supernatant was applied to a 1 ml Protino® Gluthathione Agarose 4B, and affinity purification was conducted according to the manufacturer's instructions (Macherey-Nagel, Düren, Germany). The LPOR protein was liberated from the N-terminal glutathione S-transferase tag by on-column PreScission protease treatment (20 U).

BchE-dependent conversion of Mg-PME into chlorophyllide

The reaction product of the *in vitro* BchE activity assay was further converted as follows. Purified LPOR from *D. shibae* (3.3 µM) and NADPH (2 mM) were added after completion of the BchE-dependent reaction and the resulting mixture was exposed to blue light for 2 min [38] to facilitate light-dependent LPOR catalysis. Subsequently, the assay was stopped, extracted and the formation of chlorophyllide (8-vinyl and/or 8-ethyl chlorophyllide) was spectroscopically analyzed as detailed for the *in vitro* activity assay above.

HPLC analysis of the tetrapyrrolic reaction products

The HPLC system consisted of pump PU-1518, gradient unit LG-1580-04, autosampler AS-1555, column oven X-LC, fluorescence detector FP-1520 and multiwavelength detector MD-1515 (Jasco, Tokyo, Japan). Tetrapyrrolic BchE reaction products were analyzed as described under [39] on a Nucleososil 100 C_{18} column (5 µm, 200 x 4.6 mm) using authentic reference samples (see above).

^{18}O labeling of BchE reaction products

For the labelling of reaction products, the *in vitro* BchE activity assay was modified as follows. *R. capsulatus* ZY6 (*bchH*¯) cells from a culture volume of 200 ml were suspended in 250 µl 97% $H_2{}^{18}O$ (Sigma-Aldrich, St. Louis, USA) and 25 µl of a 1 M HEPES solution, pH 7.5 were added (resulting $H_2{}^{18}O$ content: ~ 20%). Pigments were extracted (see above), dried in a stream of nitrogen and dissolved in 20 µl methanol. The resulting mixture was separated by thin layer chromatography [33]. An authentic Pchlide sample was processed in parallel which allowed for the localization and scraping of BchE reaction products from the silica plate. The silica gel was extracted with methanol and ^{18}O labeled reaction products were identified in parallel with the related unlabelled products by electrospray ionization tandem mass spectroscopy using a Fusion mass spectrometer (Thermo Scientific, Bremen, Germany) as described in [40].

Subcellular localization of BchE

Polyclonal rabbit antibodies were raised against three different epitopes using synthetic BchE peptides (CQAAPTVKDIDSLKPD, YRDRDLLKFYREAGLC and CAEAQVADWEAAADRSRK) followed by immunoaffinity purification (Metabion, Steinkirchen, Germany). Wild-type *R. capsulatus* SB1003 cells (or *R. capsulatus* ZY6 (*bchH*¯)) from a 10 ml culture were lysed (FastPrep®-24 homogenizer, 4 times at 4 m/s for 30 s) and residual unbroken cells were sedimented by low speed centrifugation (10 min, 4`000 x g). The soluble fraction was separated from the insoluble membrane fraction by

ultracentrifugation (1 h at 110`000 x g) [41]. Samples from all fractions (pellet fraction solubilized in 8 M urea) were collected for subsequent SDS-PAGE and Western blot analyses using BchE-specific antibodies and a secondary Anti-Rabbit IgG Alkaline Phosphatase antibody conjugate (Sigma, St. Louis, Missouri USA).

Subcellular localization of components essential for BchE activity

The *in vitro* BchE activity assay was modified as follows. Quantitatively disrupted *R. capsulatus* ZY6 (*bchH*¯) cells were fractionated by a single centrifugation step (12´000 g, 15 min). Activity assays were performed using either the soluble or the insoluble fraction. Alternatively, both fractions were recombined for activity measurements (reconstituted assay). Furthermore, residual soluble components were removed from the insoluble fraction by an additional washing step (150 µl 100 mM HEPES, pH 7.5, 12´000 x g, 15 min) before the enzymatic BchE activity was assessed. The reconstituted assay was also performed in the presence of soluble fractions which were obtained from *E. coli* BL21 or *R. capsulatus* DB575 (*bchE* ¯) cells as described above. The same assay was also performed with fractions from a size-fractionated soluble extract. For this purpose ultrafiltrates using 3, 10 and 30 kDa Amicon Ultra-0.5 Centrifugal Filters (Merck, Darmstadt, Germany) were obtained from the soluble fraction of *R. capsulatus* ZY6 (*bchH*¯). A reconstituted assay was performed by combining the <3 kDa, <10 kDa and <30 kDa filtrates with the insoluble fraction, respectively. Alternatively, a heat inactivated soluble fraction (10 min at 95°C) was subjected to the reconstituted assay. For each set of experiments, the activity of the *in vitro* activity was determined (100% activity). Negative controls solely contained 100 mM Hepes pH 7.5 (0% activity). All obtained results were related to these values. Representative blots from experiments performed in triplicate are shown. All results were reproduced three times.

Construction of the pRhoKs_Gm vector

An additional resistance gene was inserted into vector pRhoKs [42] to subsequently establish the *in vivo* complementation assay. The gentamicin 3-acetyltransferase gene (GenBank: AFV59818.1) was PCR-amplified from the vector pSEVA634 [43] using primers 3 and 4 (Table S2) and subsequently cloned into the *Nde*I and *BamH*I sites of pRhoKs to generate pRhoKs_Gm.

Site directed mutagenesis of *bchE*

The *bchE* gene was PCR-amplified from *R. capsulatus* SB1003 cells using primers 5 and 7 and ligated into the *BamH*I and *Xho*I sites of vector pGEX-6P-1 (GE Healthcare, Chicago, US). Mutagenesis of the *bchE* gene was performed using the QuikChange II Site-directed mutagenesis system (Agilent Technologies, Santa Clara, USA) according to manufacturer's guidance using primers 8-31 (Table S2). Modified *bchE* genes were subsequently cloned into the *Sac*I and *Xho*I sites of vector pRhoKs_Gm using primers 6 and 7 yielding plasmid pRhoKs_Gm_*bchE* and related derivatives listed in supplemental Table S1 and S2. Employed forward primers also encoded a ribosomal binding site which preceded the *bchE* gene.

Diparental mating of *R. capsulatus*

Plasmid pRhoKs_Gm_*bchE* and related derivatives were transferred into *R. capsulatus* DB575 (*BchE*¯) cells *via* conjugation using *E. coli* ST18 as a donor. Plasmids were transformed into RbCl competent *E. coli* ST18 cells [44]. Donor and recipient strains were individually grown to an OD_{578} (*E. coli*) and OD_{660} (*R. capsulatus*) of 0.5. Then the donor culture (1.8 ml) and the culture of the recipient strain (0.2 ml) were carefully mixed and sedimented by centrifugation. The cell pellet was resuspended in 100 µl PY medium containing 50 µg/ml 5-aminolevulinic acid and subsequently drops of 10 µl volume were placed on PY agar. After 24 h incubation at 30°C the cells from each drop were scraped from the plate and washed with 1 ml RCV. Cells were plated on solid RCV medium containing 1 µg/ml gentamycin to counter-select against the donor [44] and incubated at 30°C until colonies of *R. capsulatus* appeared (2-7 days) [44]. The resulting complemented strain (and all variants) were verified as follows. Presence of pRhoKs_Gm_*bchE* plasmids was demonstrated by PCR using primers 6 and 7. Translation of equal amounts of BchE (or of variant BchE) was examined from SDS-PAGE samples which were subjected to Western blotting and immunodetection using BchE specific antibodies (cultivation see below).

***In vivo* BchE complementation assay**

R. capsulatus DB575 (*BchE*¯), complemented with plasmids encoding BchE or one of the 24 variant BchE proteins or a negative control in the presence of the empty pRhoKs_Gm vector were cultivated in 5 ml RCV 2/3 PY (1 µg/ml Gm, start OD_{660} of 0.05). After 24 hours of cultivation the OD_{660} was determined and a culture volume of 1 ml was harvested by centrifugation (12´000 g, 5 min). Sedimented cells were resuspended in varying amounts of dH_2O to yield a final OD_{660} of 10. Hundred µl of the respective cell suspension were vigorously mixed with 400 µl acetone for pigment extraction [34]. After a subsequent centrifugation step (12´000 x g, 10 min), resulting supernatants were subjected to UV-visible absorption spectroscopy and the cellular BChl *a* content was determined according to the absorption maximum at 772 nm (ε_{772} = 69.0 mM^{-1} cm^{-1} [45]). All samples were subsequently extracted by the addition of 150 µl hexane (under vigorous mixing) to assess the amount of Mg-PME in the absence of BChl *a*. The resulting (lower) acetone phase was analyzed spectroscopically and the amount of Mg-PME was quantified at 415 nm (an ε_{415} = 237 mM^{-1} cm^{-1} was estimated according to value ε_{552} = 18.5 mM^{-1} cm^{-1} [34]). The resulting BChl *a* signal from the wild-type complementation and the amount of Mg-PME from the negative control (in the presence of the empty pRhoKs_Gm vector) were set to 100%. *In vivo* activity of all variant BchE proteins were related to these values. UV-visible spectra were recorded from 250 – 800 nm on a V-650 instrument (Jasco, Tokyo, Japan).

Results

Overproduction and purification of the BchE substrate Mg-PME

The *bchE*-deficient *R. capsulatus* DB575 strain (*bchE*¯) has been described as Mg-PME accumulating before (mixture of 8-vinyl and 8-ethyl Mg-PME) [34]. The overall yield of the red pigment was substantially increased by cell cultivation in the presence of 0.2% (w/v) Tween 80. The presence of the detergent facilitated the extracellular accumulation of Mg-PME as recently reported also for the production of chlorophyllide [33]. Approximately 95% of the produced pigment was purified from the supernatant of the cell culture. Hydrophobic Mg-PME was immobilized on a SepPak C_{18} cartridge and specific product elution using an acetone gradient was monitored by fluorescence spectroscopy (λ_{ex} = 438 nm, λ_{em} = 595). Fractions with an emission ratio 595 nm / 633 nm < 3.5 were discarded since other biosynthetic intermediates like PPIX gave rise to the respective fluorescence signals. In Figure 2A the fluorescence spectrum of the purified Mg-PME is shown (*black line*). Overall, 4.5 mg of the purified pigment were obtained from 1 l culture medium.

In vitro BchE activity assay

Various strategies were used to overproduce and purify BchE in our laboratory. *E. coli*, *Bacillus megaterium* or *Vibrio natrigens* were employed as production hosts. Furthermore, enhanced cobalamin supply during production, various affinity tags and different iron sulphur cluster and cobalamin cofactor reconstitution techniques were tested. Nevertheless, purified recombinant BchE only showed minimal iron content and no spectroscopic signal related to a cobalamin cofactor. Additionally, we pursued the reconstitution of the BChl *a* biosynthetic pathway in *E. coli* by analogy to a recent investigation for the oxygen-dependent cyclase AcsF [4], but the respective *E. coli* strain did not support detectable BchE activity in the presence of cobalamin *in vivo*. We concluded that the native folding and cofactor maturation machinery and/or the presence of a BchE-specific electron donor might be a prerequisite for enzymatic cyclase activity.

According to this, an *in vitro* BchE activity assay was developed which circumvented many obstacles of BchE radical SAM chemistry. The *R. capsulatus bchH*¯ mutant strain (ZY6) [36], contains a defective magnesium chelatase which leads to complete blockage of the overall BChl *a* biosynthetic pathway (Figure 1 and 2A, *grey line*). As judged from the *R. capsulatus* genome [46], no downstream effect on the functional expression of *bchE* had to be expected. A BchE *in vitro* activity assay was developed using a cell-free cellular extract of the *R. capsulatus bchH*¯ strain. Experiments were performed under strict anoxic conditions and contained high concentrations of the reducing equivalent NADPH (2 mM) and of the cofactor SAM (2 mM). Purified Mg-PME (140 µM) was used as a substrate. Under these conditions, BchE in the cell-free extract converted the red pigment Mg-PME with high efficiency into

Pchlide as indicated by a dominant fluorescence maximum at 633 nm [35] (Figure 2A, *green line*, `BchE´). Control reactions, in the absence of Mg-PME (*grey line*, `BchE` - Mg-PME) or in the absence of the cell-free *bchH*¯ extract (*black line*, background; spectrum of purified Mg-PME) failed to form Pchlide. The additional fluorescence peak for Pchlide at 633 nm was also absent when the activity assay was performed with a BchE-depleted cell-free extract which was prepared from the *R. capsulatus bchE*¯ strain DB575 (*blue line*, `BchE¯`). The employed experimental conditions enabled for the robust determination of enzymatic BchE activity. No further conversion of the BchE reaction product was determined spectroscopically.

BchE-dependent conversion of Mg-PME into chlorophyllide

Detailed spectroscopic data for the postulated intermediates of BchE catalysis (e.g. hydroxy-Mg-PME, keto-Mg-PME, Figure 1) are not available in the literature. To confirm ultimate emergence of Pchlide, we intended to convert the reaction product of the *in vitro* activity assay into the BChl *a* biosynthetic intermediate chlorophyllide. For that purpose, a recombinant production system for the light-dependent Pchlide oxidoreductase (LPOR) from *Dinoroseobacter shibae* DFL 12 was established. The target protein was affinity-purified and subsequently liberated from the N-terminal glutathione S-transferase tag by protease treatment (Figure 2A, *inlet*). When the BchE *in vitro* activity assay was supplemented with 3.3 µM of the purified LPOR protein, light-dependent depletion of the signal at 633 nm and concurrent appearance of a new fluorescence maximum at 670 nm was observed (Figure 2A, *dotted green line*, `BchE` + LPOR). A similar maximum was also obtained when an authentic Pchlide sample (mixture of 8-ethyl Pchlide and 8-vinyl Pchlide, [35]) was converted into chlorophyllide using a standard LPOR activity assay (Figure S1) as recently detailed [38]. These experiments might indicate that the *in vitro* BchE assay sustained the conversion of Mg-PME into Pchlide. It is well established that several enzymes of the BChl *a* pathway are capable of processing 8-ethyl and 8-vinyl derivatives [47] of the respective pathway intermediates [23, 48-50] as indicated in Figure 1 (substituent R is either ethyl or vinyl). HPLC analyses of the BchE reaction product(s) revealed the formation of Pchlide (8-ethyl substituent) with a retention time of 19.2 min and the parallel appearance of 8-vinyl Pchlide at 20.3 min (compare Figure 2B, *top and bottom*). These findings might indicate that BchE possess a broadened substrate specificity for the 8-ethyl and 8-vinyl derivative of Mg-PME. This hypothesises is in agreement with previously characterized pathway intermediates of BChl *a* biosynthetic mutant strains [51, 52]. However, product heterogeneity as a result of 8-vinyl reductase activity of the cell extract cannot be excluded from the present experimental strategy.

$H_2{}^{18}O$-based labelling of the BchE reaction product Pchlide

Early whole cell feeding experiments using $^{18}O_2$ and $H_2{}^{18}O$ allowed for the elucidation of the AcsF *versus* BchE-dependent biosynthetic pathways in different organisms [17, 20]. The established *in vitro* activity assay in combination with tandem mass spectrometry (MS/MS) was used to verify the origin of the carbonyl oxygen (C-13^1-oxo) of the isocyclic ring of Pchlide. A BchE assay with an overall $H_2{}^{18}O$

content of ~ 20% (v/v) was used for the parallel identification of unlabeled and ^{18}O-labeled reaction products. The positive ion electrospray mass spectrum (Figure 2C-E) unequivocally identified 8-ethyl Pchlide (m/z 591.2598, calculated m/z 591.2602; $C_{35}H_{35}N_4O_5^+$) and mono-^{18}O-labeled 8-ethyl Pchlide (m/z 593.2638, calculated m/z 593.2644). Upon collision induced dissociation, a similar fragmentation behaviour (loss of acetic acid, followed by CO_2) was shown (compare MS/MS spectra for Pchlide panel D and ^{18}O-labeled Pchlide panel E). In accordance with our HPLC analysis, weaker signals at m/z 589.2442 and 591.2484 were also observed which correspond to the 8-vinyl derivative of Pchlide and ^{18}O-labeled 8-vinyl Pchlide. From these data we conclude that the carbonyl oxygen at C-13^1 derives from a water molecule in agreement with earlier whole cell feeding experiments [20].

BchE is a radical SAM enzyme

The *in vitro* activity assay was used to investigate the main cofactor requirements of BchE. From bioinformatics analyses, radical SAM chemistry was proposed for the sophisticated catalysis of BchE. This type of reaction is initiated by the reductive cleavage of a SAM molecule which acts as a ligand of an oxygen-labile [4Fe-4S] cluster [53]. As expected, the presence of molecular oxygen or of the iron chelating agents EDTA and 2,2´-bipyridyl completely abolished BchE activity (Figure 3A). BchE *in vitro* activity was clearly stimulated with increasing SAM concentrations (maximum activity at ~6 mM SAM, Figure 3B). By contrast, addition of varying concentrations of the cofactor analogue S-adenosylhomocysteine (SAH), to an assay with 2 mM SAM, revealed an inhibitory effect on BchE catalysis as recently described for other enzymes of the radical SAM superfamily (e.g. ThiC [54]). A reduction by ~50% was observed in the presence of 750 µM SAH (Figure 3C). These findings suggested the presence of a catalytically essential [4Fe-4S] cluster and the consumption of the SAM cofactor during enzymatic turnover.

Next, NADPH and NADH were tested for their electron donor capacities. Maximum BchE activity was determined in the presence of ~1 mM NADPH. By contrast, addition of 2 mM NADH did not support Pchlide formation (Figure 3D). Radical SAM chemistry is typically initiated by one-electron transfer reactions from e.g. flavodoxins or from a specific reductase [53]. Therefore, NADPH might function as an indirect two-electron donor which fosters the reductive activation of SAM *via* additional redox components of the employed cellular extract of the *R. capsulatus bchH*$^-$ mutant strain.

With respect to the proposed cobalamin cofactor of BchE, no increase of the enzymatic activity was determined when cyano-cobalamin, adenosyl-cobalamin or hydroxo-cobalamin (0.1-1 mM) was used as a supplement of the *in vitro* activity assay. These findings might indicate that cobalamin acts as a tightly bound prosthetic group without the need to be regenerated in the employed activity assay. Accordingly, presence of the proposed cofactor binding site was addressed on the basis of an extensive mutagenesis study (see below).

Subcellular localization of BchE

Bioinformatics-based amino acid sequence analyses [26, 55] did not indicate the presence of transmembrane helices. In order to determine the subcellular localization of BchE, cell-free extracts of *R. capsulatus* wild-type cells were fractionated into in a soluble and an insoluble fraction *via* ultracentrifugation. The location of BchE was determined using polyclonal antibodies raised against three different BchE epitopes. The immunoblot depicted in Figure 4A *left* indicated a clear BchE signal from the crude cellular extract (*lane* 1). Residual unbroken cells were removed by low speed centrifugation and the membrane fractionation and the cytosolic fraction was obtained after ultracentrifugation. BchE was clearly located in the membrane fraction and only minimum amounts of BchE were detectable in the soluble fraction (compare *lanes 3* and *2* respectively). Identical results were obtained for the subcellular fractionation of cells from the *bchH*$^{-}$ mutant strain. Accordingly, the *in vitro* activity assay was gradually modified (by different fractionation techniques) to explore the potential contribution of additional (redox) components for the activity of BchE.

Membrane localized BchE requires an additional cytosolic component for activity

Cells of the *bchH*$^{-}$ strain were disrupted and subsequently fractionated by a single centrifugation step as outlined above. The soluble cytosolic fraction did not support detectable BchE activity in full agreement with the above mentioned immunoblotting experiments, where almost no BchE was found in the soluble fraction (Figure 4A *left*). When compared to the standard *in vitro* activity assay (*positive control*), residual BchE activity of 55% was obtained for the washed (150 µl 100 mM HEPES, pH 7.5) insoluble fraction (Figure 4B, *washed insoluble fraction*). When this fraction was further processed by one additional washing step, the residual BchE activity substantially decreased to 30% (*2x washed insoluble fraction*). From these experiments, we hypothesized that the additional washing step results in the depletion of residual soluble (redox) components which are essential for the activity of BchE.

This hypothesis was substantiated when the insoluble BchE fraction after one or two washing steps was recombined with the soluble cytosolic fraction. BchE activity was restored to values of 95 and 85%, respectively (Figure 4B, e.g. *washed insoluble fraction + soluble fraction*). Successful reconstitution of BchE activity was also observed when the soluble fraction of the enzymatically inactive *bchE*$^{-}$ mutant strain was used as a supplement. From these experiments we concluded that the membrane localized BchE protein requires an additional soluble component (or components) for the synthesis of Pchlide.

Interestingly, substantial decrease of the BchE activity was observed when the *in vitro* assay was performed in the presence of increasing concentrations of the non-ionic detergent Triton X-100 (60 and 5% residual activity using 0.06 and 0.25% (v/v) detergent) (Figure 4A *right*). The presence of detergent might hamper the interplay of BchE with additional (soluble) redox components at the membrane/cytoplasm interface. To further explore the nature of the required soluble component(s) we made use of a heterologous activity assay and size fractionation experiments.

BchE activity is not sustained by a soluble extract from E. coli

Radical SAM enzymes often require specific single electron donors (and acceptors) for activity [53]. These redox proteins, e.g. flavodoxins, often show a broad specificity which also allows for the heterologous electron transfer between redox proteins from different sources.

BchE activity experiments using the insoluble BchE-containing fraction were supplemented with the soluble cytoplasmic fraction that was prepared from wild-type *E. coli* cells. The resulting chimeric BchE assay did not restore BchE activity (Figure 4C, *washed insoluble fraction + soluble E. coli fraction*). These experiments probably indicate that BchE catalysis relies on *R. capsulatus* specific soluble component(s) which were not supplied by the employed *E. coli* extract. This finding might explain that our initial attempts to reconstitute the overall BChl *a* biosynthesis pathway in *E. coli* were unsuccessful.

Size fractionation of the soluble R. capsulatus extract

To roughly estimate the molecular weight of the additional BchE component(s), soluble *R. capsulatus* extracts were size fractionated by ultrafiltration using membranes with a 3 kDa, 10 kDa and 30 kDa cut-offs, respectively. BchE activity assays in the presence of the insoluble fraction were then complemented by addition of the respective filtrates. As indicated in Figure 4C, a <30 kDa and a <10 kDa filtrate was able to restore BchE activity to the same extent as the unfractionated soluble extract (e.g. *washed insoluble fraction + soluble fraction < 10 kDa*). By contrast, the < 3 kDa filtrate did not facilitate for enzymatic activity. This was also the case when a heat inactivated (10 min, 95°C) unfractionated soluble extract was analyzed instead (*washed insoluble fraction + heat inactivated soluble fraction*). These findings show that membrane localized BchE catalysis requires a temperature-sensitive soluble component (or components) with an estimated molecular mass between 3 kDa and 10 kDa. However, the exact upper limit of 10 kDa must be judged carefully as the <10 kDa filtrate revealed a series of uncharacterized proteins with a higher molecular weight. Proteomics analysis of the <10 kDa filtrate revealed more than 100 potential proteins. Among these candidates, two redox proteins (ferredoxins with gene ID 31491607 and 31491235R) were overproduced in *E. coli*. However, soluble extracts containing the overproduced proteins did not allow for the reconstitution of BchE activity.

Characterization of BchE cofactor binding sites

Structure guided mutagenesis is a versatile tool for the molecular understanding of distantly related enzymes. The present protein data bank solely contains the structure of OxsB as a homologous radical SAM protein with a bound cobalamin cofactor (PDB code: 5UL3, 18.2% sequence identity). The OxsB coordinates were used in a structural modelling approach to investigate the proposed cofactor requirements of BchE. The tentative structural BchE model comprising residues 1–433 (out of 575 residues) was calculated using the SWISS-MODEL server [29] and is depicted in Figure 5. The hypothetical model contains the N-terminal cobalamin binding domain (residues 1-196) displayed in green, the adenosylmethionine (AdoMet) radical domain 197-412 in light blue which is followed by a

C-terminal helix in orange. Based on this tentative structural model, highly conserved BchE residues were identified and categorized as follows (related OxsB residues in brackets):

(i) potential ligands of the [4Fe-4S] cluster in the AdoMet radical domain, which were Cys^{204} (Cys^{213}), Cys^{208} (Cys^{318}) and Cys^{211} (Cys^{321}); (ii) residues which might interact with the SAM molecule in the cluster binding region of the AdoMet domain, which were Phe^{210} (Phe^{320}), Glu^{308} (Glu^{436}) and Lys^{320} (Lys^{448}); (iii) amino acids that might be part of the lower cobalamin binding pocket that potentially interact with the corrin ring system, which were Asp^{248} (Ala^{361}), Glu^{249} (Glu^{363}); (iv) residues that might be a part of the upper cobalamin binding pocket that potentially harbours the dimethylbenzimidazole moiety of the cofactor, which were Leu^{29} (Leu^{143}), Thr^{71} (Ser^{184}), Val^{97}(Thr^{214}), Glu^{126} (Glu^{242}) and Arg^{202} (Arg^{311}) and (v) highly conserved residues on the potential BchE surface Glu^{250} (Asp^{324}) and Trp^{214} (Asp^{324}) that do not have a direct counterpart in OxsB.

In the homology model presented in Figure 5, the respective amino acid residues of BchE are highlighted as yellow sticks and the supposed cofactors (SAM in *pale pink*, the ligated iron sulfur cluster as *spheres*, Cbl in *blue*) were superimposed according to the structure of OxsB. Functional relevance of these 15 amino acid positions was explored in a comprehensive mutagenesis approach. The majority of these residues was replaced by a conservative amino acid exchange and subsequently a more drastic amino acid exchange was explored.

To assess the impact of individual amino acid exchanges on BchE activity an *in vivo* complementation assay was established. For this purpose, the broad-host vector pRhoKs [42] was modified by the addition of the gentamicin-3-acetyltransferase (GenBank: AFV59818.1) resistance gene which allowed for the stable replication of the vector in the genetic background of the *R. capsulatus bchE*¯ strain. An overall of 24 mutagenized *bchE* genes were cloned into the modified vector under control of the constitutive *aphII* promotor. Subsequently, all plasmids were transferred into the *R. capsulatus bchE*¯ strain by diparental mating and the presence of complementing *bchE* gene was verified by PCR. The strains were cultivated under microaerophilic conditions and the formation of identical amounts of BchE was verified by Western blot analyses.

Enzymatic BchE activity of each complemented strain was analyzed by two different extraction methods followed by absorption spectroscopy. The amount of BChl *a* and of Mg-PME was determined by the absorption maxima at 772 nm and 415 nm. Figure 6 clearly indicates the presence of high amounts of BChl *a* (~0.95 nmol per 1 ml culture with an OD_{660} = 1) for the complemented strain. By contrast, the mutant strain (in the presence of the empty pRhoKs vector) was devoid of BChl *a* and showed substantial accumulation of Mg-PME (~0.81 nmol per 1 ml culture with an OD_{660} = 1). All strains with a decreased BChl *a* content showed the accumulation of Mg-PME. Accordingly, the cellular BChl *a* content can be used as an effective measure of the enzymatic activity of all BchE variants. For the investigation of the various proposed binding sites, we obtained the following results:

(i) The proposed [4Fe-4S] cluster mutants C204A, C208A and C211A did not reveal detectable BchE activity, which is in full agreement with the proposed radical SAM chemistry of BchE.

(ii) Mutants F210W, E308Q, E308K, K320Q and K320R did not show detectable BchE activity. Solely the conservative exchange of F210L revealed a residual BchE activity of ~6%. These findings support a key catalytic role of residues Phe^{210}, Glu^{308} and Lys^{320} which might be consistent with the proposed ligation of the AdoMet (SAM) molecule in the cluster binding region of the AdoMet domain.
(iii) BchE variants D248N, D248A, E249Q and E249K revealed no BchE activity. As judged from the related OxsB structure, residues Asp^{248} and Glu^{249} might be involved in the binding of the corrin ring structure of the proposed cobalamin cofactor of BchE.
(iv) BchE residues Leu^{29}, Thr^{71}, Val^{97} were hypothesized as part of the dimethylbenzimidazole binding pocket. Mutations L29M, T71A and V97M revealed substantial residual activities of 42%, 30% and 25%, respectively. These conservative exchanges might not block this part of the proposed cobalamin bonding site efficiently. By contrast, introduction of spatially more demanding residues in variants L29R, T71K and V97R completely abolished BChl *a* synthesis. These findings are in agreement with residues Leu^{29}, Thr^{71} and Val^{97} as part of a hydrophobic cofactor binding pocket. Within the cobalamin binding site of OxsB a conserved glutamate and arginine delineate the ribose moiety of the cofactor. The related BchE mutants E126K and R202E indicate only residual activities of ~4% and ~2% for the synthesis of BChl *a*, accompanied by a massive increase of Mg-PME. These findings clearly indicate a substantial role of residues Glu^{126} and Arg^{202} in agreement with a related function as described for OxsB.
(v) The highly conserved BchE residues Trp^{214} and Glu^{363} do not have a direct counterpart in OxsB. Both residues can be found at the surface of the modeled structure of BchE, which argues against a functional role in cofactor or substrate interaction. The BchE variant W214S revealed only ~11% residual activity whereas the related protein W214K and also E250K failed to produce detectable amounts of BChl *a*. From these data, central relevance of Trp^{214} and Glu^{363} for BchE activity was concluded and a potential role for the `docking` of a BchE-related redox protein was hypothesized. From the overall mutagenesis study, we conclude that BchE contains a cobalamin binding site in close analogy to OxsB. This result of our molecular investigation is in full agreement with preceding *in vivo* studies of cobalamin-requiring mutant strains [23].

Discussion

Tetrapyrrolic compounds chlorophyll *a* or BChl *a* are among the most abundant pigments on our planet [56]. The isocyclic E-ring clearly distinguishes these pigments from other tetrapyrroles such as heme or cobalamin since this part of the macrocycle is of central importance for the unique light-harvesting properties of these molecules. In the last decades, our knowledge on the biosynthesis of different types of chlorophylls has constantly increased at the biochemical and also on the structural level. However, the enzymology of the oxygen-dependent or oxygen-independent cyclase is a clear exception. Neither the catalysis of AcsF nor the BchE-dependent formation of Pchlide has been elucidated mechanistically.

BchE belongs to a subset of proteins from the radical SAM superfamily which contain a cobalamin binding domain at the N-terminus. Among these, PhpK (21% sequence identity) catalyzes the methylation of a phosphinate group, TsrM (20% sequence identity) enables the synthesis of 2-methyltryptophan form tryptophan and GenK (27% sequence identity) facilitates the C-6´methylation during the biosynthesis of gentamicin [57]. These cobalamin-dependent radical SAM enzymes all catalyze the methylation of unreactive carbon or phosphorus atoms. To date, the initially characterized OxsB is the only radical SAM protein which makes use of an additional cobalamin cofactor in a non-methyltransferase reaction. The solved OxsB crystal structure is a suitable template for the elucidation of the main cofactor requirements of BchE in a structure guided mutagenesis approach. However, it must be clear that this model system only facilitates the oxidative 2 e^- ring contraction of the substrate 2´-deoxyadenosine phosphate. Therefore, OxsB catalysis might parallel the initial (activating) steps of BchE catalysis but this homologous protein will not serve as model system for the overall 6 e^- oxidative cyclization and `oxygenation` that is catalyzed by BchE.

The present investigation makes use of an *in vitro* activity assay which is based on biotechnologically produced Mg-PME and a cell-free extract of the *R. capsulatus bchH*$^-$ mutant. This strain provides robust BchE activity and allows for the spectroscopic determination of evolving Pchlide in the absence of interfering fluorescence signals from other BChl *a* biosynthetic intermediates. The assay was verified by HPLC and isotope label transfer experiments and revealed that the oxygen atom of the C-13^1-oxo group is derived from a water molecule. Radical SAM chemistry of BchE has been proposed on the basis of computational analyses [22]. This was confirmed since BchE activity was stimulated by increasing concentrations of SAM or NADPH and clear inhibition in the presence of the SAM analog S-adenosylhomocysteine was shown. These findings are in agreement with recently discussed enzymatic mechanisms of BchE which predicted the requirement for three equivalents of SAM to produce each molecule of Pchlide [3].

Our efforts towards the entire reconstitution of the radical SAM reaction of BchE were always unsuccessful. Maturation of the [4Fe-4S] cluster with parallel incorporation of the cobalamin might be the main hurdle during recombinant BchE overproduction. To date, our alternative approaches towards the *in vitro* reconstitution of the [4Fe-4S] cluster in the presence of cobalamin were not successful. In the present literature, only the recombinant production and purification of a urea-solubilized BchE fragment from *Rubrivivax gelatinosus* has been demonstrated [21]. Related UV-visible spectral analyses suggested the presence of a [Fe-S] cluster but no additional cobalamin signal was detectable.

The reconstitution of BchE activity poses further challenges which go beyond the production of functional BchE. Radical SAM enzyme activity is only observed when the reductive cleavage of SAM is efficiently initiated by an electron donor. In many cases, presence of the natural electron donor is required (e.g. a specific flavodoxin/flavodoxin oxidoreductase system) since an artificial electron donor (e.g. dithionite) is only able to partially sustain enzyme activity [53]. Furthermore, an additional mediator might be needed (e.g. methyl viologen or benzyl viologen [58]) when the radical SAM reaction

is initiated in the presence of a ´chemical reductant´. Radical SAM catalytic reaction cycles can also include the reductive or oxidative quenching of evolving product radicals which then necessitates an (extra) electron donor or acceptor. From the present literature it is evident that non-physiological conditions often frustrate radical SAM enzyme activity and may lead to abortive SAM cleavage [59] or may result in enzymatic reactions with altered regiospecificity [3]. Even well-studied systems show poor turnover with only a few number of turnover events per protein [53].

Based on the localization experiments of the present investigation, it was demonstrated that BchE is a membrane-bound protein. Theoretical analyses did not indicate the presence of membrane helices which might indicate that BchE is functional as a peripheral membrane protein. In line with this hypothesis, complete loss of enzymatic activity was observed when the activity assay was performed in the presence of detergent. BchE also requires (an) additional soluble component(s) for activity. Size-fractionation experiments pointed towards a small *R. capsulatus* protein which might function as specific electron donor or acceptor of BchE. Dithionite has been successfully used as an artificial electron donor of a large number of radical SAM enzymes [53]. With respect to BchE it is quite clear that a cyclase-specific reduction system is required. Such a BchE-specific redox protein might be the central component of the employed soluble extract of the established *in vitro* activity assay. Besides this, the radical SAM reaction of BchE might also include the reductive or oxidative quenching of an evolving product radical which then necessitates for an additional electron donor or acceptor. This might hamper the identification of BchE interaction partners on the basis of activity experiments in the future.

The requirement for a cobalamin cofactor for BchE catalysis was exemplified on the basis of cobalamin-requiring mutant strains [23, 60, 61]. An *in vivo* complementation assay was established, aiming to characterize site-directed BchE variants which impede the binding of the cobalamin cofactor or the radical SAM [4Fe-4S] cluster. The structure guided mutagenesis study suggested strong functional conservation of the key residues of OxsB and BchE with Cys^{204}, Cys^{208} and Cys^{211} as ligands of the radical SAM [4Fe-4S] cluster, with involvement of Phe^{210}, Glu^{308} and Lys^{320} in the binding of SAM and with Asp^{248}, Glu^{249}, Leu^{29}, Thr^{71} and Val^{97} as part of the proposed cobalamin cofactor binding pocket. These findings are in full agreement with a cobalamin-dependent radical SAM mechanism of BchE.

As a future perspective, interactomics approaches using a tagged version of BchE must be considered as a promising strategy for the identification of BchE-specific redox partner protein(s). Such efforts should be supported by comparative genomics approaches to reduce the number of candidate proteins which need to be further analyzed by classical genetic and biochemical methods. Detailed analyses of site-directed mutant strains might pave the way for the identification of a variant BchE enzyme that accumulates e.g. the proposed hydroxymethylene intermediate, the related ketone intermediate or alternatively an artificial side product of the cyclase reaction. It would be very beneficial to support these efforts by using organic chemistry for the synthesis of these (intermediate) molecules.

It is quite clear that BchE catalysis extends the repertoire of radical SAM chemistry by an unprecedented reaction. The present investigation might contribute to the future elucidation of the underlying enzyme mechanism.

Data availability statement

The theoretical BchE model is accessible on the Protein Model DataBase (PMDB): PM0083327. The amino acid and the nucleotide sequence of *R. capsulatus* BchE and *D. shibae* LPOR were obtained from the Kyoto Encyclopedia of Genes and Genomes (KEGG): RCAP_rcc00669 and Dshi_4160.

Acknowledgments:

We thank Simone Virus for her excellent technical assistance and Joshua Rumler for his support with localization experiments.

Declarations of interest: The authors declare that they have no conflicts of interest with the contents of this article.

Funding information: This work was supported by Deutsche Forschungsgemeinschaft Grants MO 1749/1-3 and JA 470/9-3

Literature

1 Bryant, D. A., Hunter, C. N. and Warren, M. J. (2020) Biosynthesis of the modified tetrapyrroles-the pigments of life. J Biol Chem. **295**, 6888-6925

2 Herbst, J., Girke, A., Hajirezaei, M. R., Hanke, G. and Grimm, B. (2018) Potential roles of YCF54 and ferredoxin-NADPH reductase for magnesium protoporphyrin monomethylester cyclase. Plant J. **94**, 485-496

3 Yokoyama, K. and Lilla, E. A. (2018) C-C bond forming radical SAM enzymes involved in the construction of carbon skeletons of cofactors and natural products. Nat Prod Rep. **35**, 660-694

4 Chen, G. E., Canniffe, D. P., Barnett, S. F. H., Hollingshead, S., Brindley, A. A., Vasilev, C., Bryant, D. A. and Hunter, C. N. (2018) Complete enzyme set for chlorophyll biosynthesis in *Escherichia coli*. Science Advances. **4**, eaaq1407

5 Willows, R. D. (2003) Biosynthesis of chlorophylls from protoporphyrin IX. Nat Prod Rep. **20**, 327-341

6 Tikh, I. B., Quin, M. B. and Schmidt-Dannert, C. (2014) A tale of two reductases: extending the bacteriochlorophyll biosynthetic pathway in *E. coli*. PLoS One. **9**, e89734

7 Boldareva-Nuianzina, E. N., Blahova, Z., Sobotka, R. and Koblizek, M. (2013) Distribution and origin of oxygen-dependent and oxygen-independent forms of Mg-protoporphyrin monomethylester cyclase among phototrophic proteobacteria. Appl Environ Microbiol. **79**, 2596-2604

8 Chen, G. E., Canniffe, D. P. and Hunter, C. N. (2017) Three classes of oxygen-dependent cyclase involved in chlorophyll and bacteriochlorophyll biosynthesis. Proc Natl Acad Sci U S A. **114**, 6280-6285

9 Tang, K. H., Wen, J., Li, X. and Blankenship, R. E. (2009) Role of the AcsF protein in *Chloroflexus aurantiacus*. J Bacteriol. **191**, 3580-3587

10 Pinta, V., Picaud, M., Reiss-Husson, F. and Astier, C. (2002) *Rubrivivax gelatinosus* acsF (previously orf358) codes for a conserved, putative binuclear-iron-cluster-containing protein involved in aerobic oxidative cyclization of Mg-protoporphyrin IX monomethylester. J Bacteriol. **184**, 746-753
11 Hollingshead, S., Kopecna, J., Jackson, P. J., Canniffe, D. P., Davison, P. A., Dickman, M. J., Sobotka, R. and Hunter, C. N. (2012) Conserved chloroplast open-reading frame ycf54 is required for activity of the magnesium protoporphyrin monomethylester oxidative cyclase in *Synechocystis* PCC 6803. J Biol Chem. **287**, 27823-27833
12 Albus, C. A., Salinas, A., Czarnecki, O., Kahlau, S., Rothbart, M., Thiele, W., Lein, W., Bock, R., Grimm, B. and Schottler, M. A. (2012) LCAA, a novel factor required for magnesium protoporphyrin monomethylester cyclase accumulation and feedback control of aminolevulinic acid biosynthesis in *tobacco*. Plant Physiol. **160**, 1923-1939
13 Bollivar, D., Braumann, I., Berendt, K., Gough, S. P. and Hansson, M. (2014) The Ycf54 protein is part of the membrane component of Mg-protoporphyrin IX monomethyl ester cyclase from barley (*Hordeum vulgare L*.). FEBS J. **281**, 2377-2386
14 Chen, G. E. and Hunter, C. N. (2020) Protochlorophyllide synthesis by recombinant cyclases from eukaryotic oxygenic phototrophs and the dependence on Ycf54. Biochem J. **477**, 2313-2325
15 Stuart, D., Sandstrom, M., Youssef, H. M., Zakhrabekova, S., Jensen, P. E., Bollivar, D. W. and Hansson, M. (2020) Aerobic Barley Mg-protoporphyrin IX Monomethyl Ester Cyclase is Powered by Electrons from Ferredoxin. Plants (Basel). **9**
16 Walker, C. J., Mansfield, K. E., Smith, K. M. and Castelfranco, P. A. (1989) Incorporation of atmospheric oxygen into the carbonyl functionality of the protochlorophyllide isocyclic ring. The Biochemical journal. **257**, 599-602
17 Porra, R. J., Schäfer, W., Gad'on, N., Katheder, I., Drews, G. and Scheer, H. (1996) Origin of the Two Carbonyl Oxygens of Bacteriochlorophyll a. European Journal of Biochemistry. **239**, 85-92
18 Kumka, J. E., Schindel, H., Fang, M., Zappa, S. and Bauer, C. E. (2017) Transcriptomic analysis of aerobic respiratory and anaerobic photosynthetic states in *Rhodobacter capsulatus* and their modulation by global redox regulators RegA, FnrL and CrtJ. Microb Genom. **3**, e000125
19 Zappa, S., Li, K. and Bauer, C. E. (2010) The tetrapyrrole biosynthetic pathway and its regulation in *Rhodobacter capsulatus*. Adv Exp Med Biol. **675**, 229-250
20 Porra, R. J., Schäfer, W., Katheder, I. and Scheer, H. (1995) The derivation of the oxygen atoms of the 13(1)-oxo and 3-acetyl groups of bacteriochlorophyll a from water in *Rhodobacter sphaeroides* cells adapting from respiratory to photosynthetic conditions: evidence for an anaerobic pathway for the formation of isocyclic ring E. FEBS Lett. **371**, 21-24
21 Ouchane, S., Steunou, A. S., Picaud, M. and Astier, C. (2004) Aerobic and anaerobic Mg-protoporphyrin monomethyl ester cyclases in purple bacteria: a strategy adopted to bypass the repressive oxygen control system. J Biol Chem. **279**, 6385-6394
22 Sofia, H. J., Chen, G., Hetzler, B. G., Reyes-Spindola, J. F. and Miller, N. E. (2001) Radical SAM, a novel protein superfamily linking unresolved steps in familiar biosynthetic pathways with radical mechanisms: functional characterization using new analysis and information visualization methods. Nucleic Acids Res. **29**, 1097-1106
23 Gough, S. P., Petersen, B. O. and Duus, J. O. (2000) Anaerobic chlorophyll isocyclic ring formation in *Rhodobacter capsulatus* requires a cobalamin cofactor. Proc Natl Acad Sci U S A. **97**, 6908-6913
24 Bridwell-Rabb, J., Zhong, A., Sun, H. G., Drennan, C. L. and Liu, H. W. (2017) A B12-dependent radical SAM enzyme involved in oxetanocin A biosynthesis. Nature. **544**, 322-326
25 Almagro Armenteros, J. J., Tsirigos, K. D., Sonderby, C. K., Petersen, T. N., Winther, O., Brunak, S., von Heijne, G. and Nielsen, H. (2019) SignalP 5.0 improves signal peptide predictions using deep neural networks. Nat Biotechnol. **37**, 420-423
26 Krogh, A., Larsson, B., von Heijne, G. and Sonnhammer, E. L. (2001) Predicting transmembrane protein topology with a hidden Markov model: application to complete genomes. J Mol Biol. **305**, 567-580

27 Altschul, S. F., Gish, W., Miller, W., Myers, E. W. and Lipman, D. J. (1990) Basic local alignment search tool. J Mol Biol. **215**, 403-410
28 Waterhouse, A. M., Procter, J. B., Martin, D. M., Clamp, M. and Barton, G. J. (2009) Jalview Version 2--a multiple sequence alignment editor and analysis workbench. Bioinformatics. **25**, 1189-1191
29 Biasini, M., Bienert, S., Waterhouse, A., Arnold, K., Studer, G., Schmidt, T., Kiefer, F., Gallo Cassarino, T., Bertoni, M., Bordoli, L. and Schwede, T. (2014) SWISS-MODEL: modelling protein tertiary and quaternary structure using evolutionary information. Nucleic Acids Res. **42**, W252-258
30 Schrödinger, L. (2010) The PyMOL Molecular Graphics System (Schrödinger, LLC, New York), Version 1.5.0.4.
31 Weaver, P. F., Wall, J. D. and Gest, H. (1975) Characterization of *Rhodopseudomonas capsulata*. Arch Microbiol. **105**, 207-216
32 Young, D. A., Bauer, C. E., Williams, J. C. and Marrs, B. L. (1989) Genetic evidence for superoperonal organization of genes for photosynthetic pigments and pigment-binding proteins in *Rhodobacter capsulatus*. Mol Gen Genet. **218**, 1-12
33 Müller, A. H., Gough, S. P., Bollivar, D. W., Meldal, M., Willows, R. D. and Hansson, M. (2011) Methods for the preparation of chlorophyllide a: an intermediate of the chlorophyll biosynthetic pathway. Anal Biochem. **419**, 271-276
34 Gough, S. P., Rzeznicka, K., Peterson Wulff, R., Francisco Jda, C., Hansson, A., Jensen, P. E. and Hansson, M. (2007) A new method for isolating physiologically active Mg-protoporphyrin monomethyl ester, the substrate of the cyclase enzyme of the chlorophyll biosynthetic pathway. Plant Physiol Biochem. **45**, 932-936
35 Heyes, D. J., Ruban, A. V., Wilks, H. M. and Hunter, C. N. (2002) Enzymology below 200 K: the kinetics and thermodynamics of the photochemistry catalyzed by protochlorophyllide oxidoreductase. Proc Natl Acad Sci U S A. **99**, 11145-11150
36 Yang, Z. M. and Bauer, C. E. (1990) *Rhodobacter capsulatus* genes involved in early steps of the bacteriochlorophyll biosynthetic pathway. J Bacteriol. **172**, 5001-5010
37 Bollivar, D. W., Jiang, Z. Y., Bauer, C. E. and Beale, S. I. (1994) Heterologous expression of the bchM gene product from *Rhodobacter capsulatus* and demonstration that it encodes S-adenosyl-L-methionine:Mg-protoporphyrin IX methyltransferase. J Bacteriol. **176**, 5290-5296
38 Kaschner, M., Loeschcke, A., Krause, J., Minh, B. Q., Heck, A., Endres, S., Svensson, V., Wirtz, A., von Haeseler, A., Jaeger, K. E., Drepper, T. and Krauss, U. (2014) Discovery of the first light-dependent protochlorophyllide oxidoreductase in anoxygenic phototrophic bacteria. Mol Microbiol. **93**, 1066-1078
39 Helfrich, M., Ross, A., King, G. C., Turner, A. G. and Larkum, A. W. (1999) Identification of [8-vinyl]-protochlorophyllide a in phototrophic prokaryotes and algae: chemical and spectroscopic properties. Biochim Biophys Acta. **1410**, 262-272
40 Walther, J., Bröcker, M. J., Wätzlich, D., Nimtz, M., Rohde, M., Jahn, D. and Moser, J. (2009) Protochlorophyllide: a new photosensitizer for the photodynamic inactivation of Gram-positive and Gram-negative bacteria. FEMS Microbiol Lett. **290**, 156-163
41 Wingfield, P. T. (2014) Preparation of Soluble Proteins from *Escherichia coli*. Curr Protoc Protein Sci. **78**, 6 2 1-6 2 22
42 Katzke, N., Arvani, S., Bergmann, R., Circolone, F., Markert, A., Svensson, V., Jaeger, K. E., Heck, A. and Drepper, T. (2010) A novel T7 RNA polymerase dependent expression system for high-level protein production in the phototrophic bacterium *Rhodobacter capsulatus*. Protein Expr Purif. **69**, 137-146
43 Martinez-Garcia, E., Aparicio, T., Goni-Moreno, A., Fraile, S. and de Lorenzo, V. (2015) SEVA 2.0: an update of the Standard European Vector Architecture for de-/re-construction of bacterial functionalities. Nucleic Acids Res. **43**, D1183-1189
44 Thoma, S. and Schobert, M. (2009) An improved *Escherichia coli* donor strain for diparental mating. FEMS Microbiol Lett. **294**, 127-132

45 Sauer, K. S., L; John R.; Schultz, A.J. (1966) The dimerization of chlorophyll a, chlorophyll b, and bacteriochlorophyll in solution. Journal of the American Chemical Society. **88 (12)**, 2681-2688
46 Strnad, H., Lapidus, A., Paces, J., Ulbrich, P., Vlcek, C., Paces, V. and Haselkorn, R. (2010) Complete genome sequence of the photosynthetic purple nonsulfur bacterium *Rhodobacter capsulatus* SB 1003. J Bacteriol. **192**, 3545-3546
47 Bröcker, M. J., Jahn, D. and Moser, J. (2012) Key Enzymes of Chlorophyll Biosynthesis. in Handbook of Porphyrin Science. **16-20**, 1-43
48 Liu, Z. and Bryant, D. A. (2011) Multiple types of 8-vinyl reductases for (bacterio)chlorophyll biosynthesis occur in many green sulfur bacteria. J Bacteriol. **193**, 4996-4998
49 Bröcker, M. J., Wätzlich, D., Uliczka, F., Virus, S., Saggu, M., Lendzian, F., Scheer, H., Rüdiger, W., Moser, J. and Jahn, D. (2008) Substrate recognition of nitrogenase-like dark operative protochlorophyllide oxidoreductase from *Prochlorococcus marinus*. J Biol Chem. **283**, 29873-29881
50 Klement, H., Helfrich, M., Oster, U., Schoch, S. and Rüdiger, W. (1999) Pigment-free NADPH:protochlorophyllide oxidoreductase from *Avena sativa L*. Purification and substrate specificity. Eur J Biochem. **265**, 862-874
51 Bollivar, D. W., Suzuki, J. Y., Beatty, J. T., Dobrowolski, J. M. and Bauer, C. E. (1994) Directed mutational analysis of bacteriochlorophyll a biosynthesis in *Rhodobacter capsulatus*. J Mol Biol. **237**, 622-640
52 Suzuki, J. Y. and Bauer, C. E. (1995) Altered monovinyl and divinyl protochlorophyllide pools in bchJ mutants of *Rhodobacter capsulatus*. Possible monovinyl substrate discrimination of light-independent protochlorophyllide reductase. J Biol Chem. **270**, 3732-3740
53 Broderick, J. B., Duffus, B. R., Duschene, K. S. and Shepard, E. M. (2014) Radical S-adenosylmethionine enzymes. Chem Rev. **114**, 4229-4317
54 Palmer, L. D. and Downs, D. M. (2013) The thiamine biosynthetic enzyme ThiC catalyzes multiple turnovers and is inhibited by S-adenosylmethionine (AdoMet) metabolites. J Biol Chem. **288**, 30693-30699
55 Sonnhammer, E. L., von Heijne, G. and Krogh, A. (1998) A hidden Markov model for predicting transmembrane helices in protein sequences. Proc Int Conf Intell Syst Mol Biol. **6**, 175-182
56 Grimm, B., Porra, R. J., Rüdiger, W. and Scheer, H. Chlorophylls and Bacteriochlorophylls Biochemistry, Biophysics, Functions and Applications
57 Kim, H. J., McCarty, R. M., Ogasawara, Y., Liu, Y. N., Mansoorabadi, S. O., LeVieux, J. and Liu, H. W. (2013) GenK-catalyzed C-6' methylation in the biosynthesis of gentamicin: isolation and characterization of a cobalamin-dependent radical SAM enzyme. J Am Chem Soc. **135**, 8093-8096
58 Bruender, N. A., Young, A. P. and Bandarian, V. (2015) Chemical and Biological Reduction of the Radical SAM Enzyme 7-Carboxy-7-deazaguanine [corrected] Synthase. Biochemistry. **54**, 2903-2910
59 Lotierzo, M., Raux, E., Tse Sum Bui, B., Goasdoue, N., Libot, F., Florentin, D., Warren, M. J. and Marquet, A. (2006) Biotin synthase mechanism: mutagenesis of the YNHNLD conserved motif. Biochemistry. **45**, 12274-12281
60 Pollich, M., Jock, S. and Klug, G. (1993) Identification of a gene required for the oxygen-regulated formation of the photosynthetic apparatus of *Rhodobacter capsulatus*. Mol Microbiol. **10**, 749-757
61 Gray, M. J. and Escalante-Semerena, J. C. (2007) Single-enzyme conversion of FMNH2 to 5,6-dimethylbenzimidazole, the lower ligand of B12. Proc Natl Acad Sci U S A. **104**, 2921-2926
62 Canniffe, D. P., Chidgey, J. W. and Hunter, C. N. (2014) Elucidation of the preferred routes of C8-vinyl reduction in chlorophyll and bacteriochlorophyll biosynthesis. Biochem J. **462**, 433-440

Abbreviations: BChl *a*, Bacteriochlorophyll *a*; DTT, Dithiothreitol; IPTG, isopropyl-β-D-thiogalactopyranoside; Mg-PME, Mg-protoporphyrin IX monomethyl ester; NDT, sodium dithionite; Pchlide, protochlorophyllide; PPIX, protoporphyrin IX; SAM, S-adenosylmethionine; SAH, S-adenosylhomocysteine.

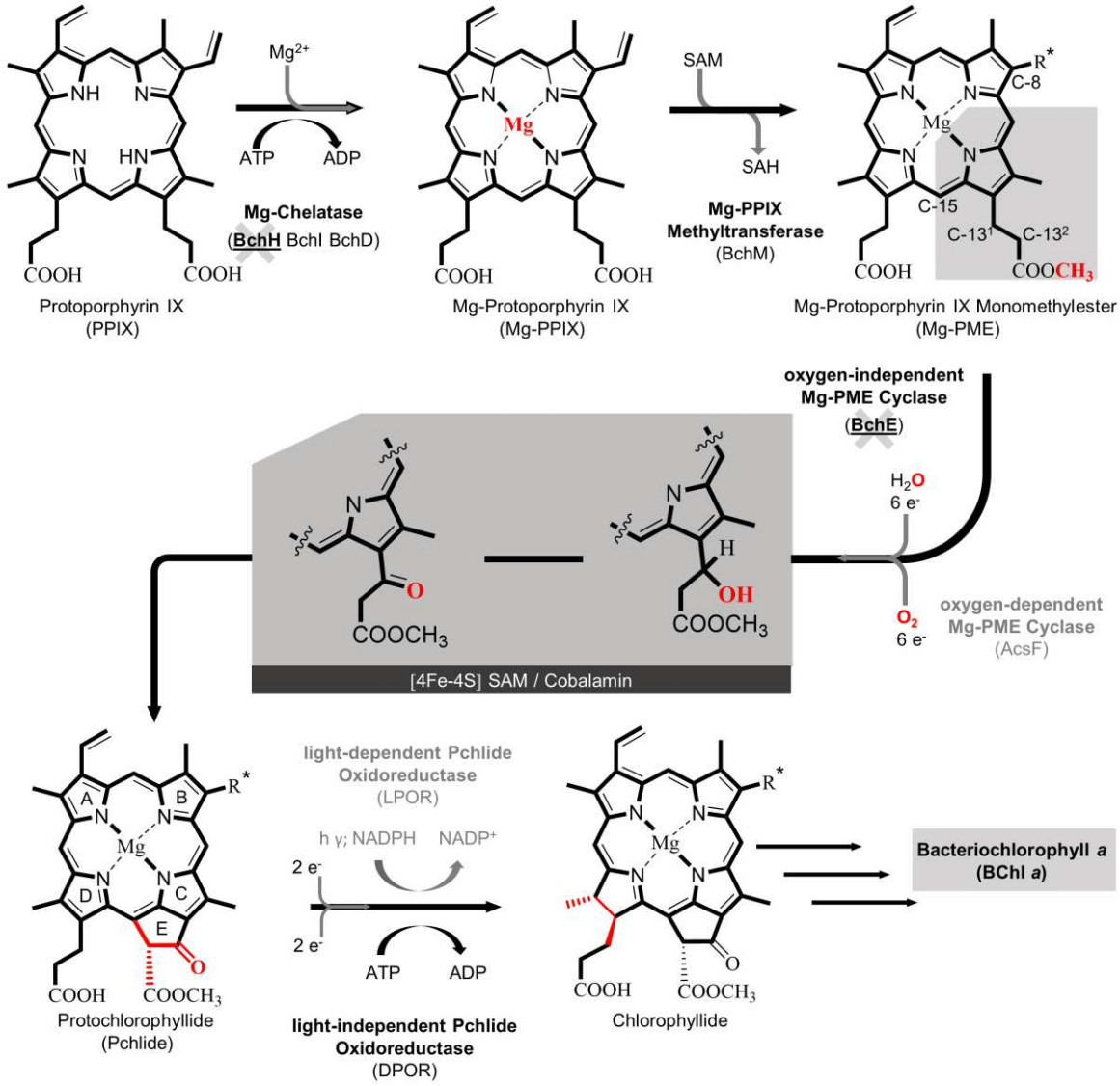

Figure 1. Central steps for the biosynthesis of BChl *a* **in *R. capsulatus* (black).**
Protoporphyrin IX (PPIX) is converted into Mg-PPIX by the magnesium chelatase complex (BchlI, BchlD, BchlH). Strain *bchH*$^-$ is completely blocked in the synthesis of BChl *a* (*crossed grey*). A BchE activity assay was established using the crude cellular extract of this mutant. Mg-PPIX is methylated by the Mg-PPIX methyltransferase (BchM). Resulting Mg-PPIX monomethyl ester (Mg-PME) is converted into protochlorophyllide (Pchlide) by the oxygen-independent Mg-PME cyclase termed BchE. Proposed reaction intermediates and cofactors are indicated. Strain *bchE*$^-$ accumulates Mg-PME, a related crude cellular extract contains a soluble component which is essential for the activity of BchE (*crossed grey*). Light-independent Pchlide oxidoreductase (DPOR) catalyzes the formation of chlorophyllide. Alternative biosynthetic enzymes which are absent in *R. capsulatus* are indicated in grey: the oxygen-dependent cyclase AcsF and the light-dependent Pchlide oxidoreductase (LPOR). R is either vinyl or ethyl. * Related enzymes were proposed to process 8-ethyl and 8-vinyl derivatives. Enzymatic reduction of the 8-vinyl group is observed at different stages of the BChl *a* pathway [6, 49, 50], 8-vinyl chlorophyllide might act as a preferred substrate of the 8-vinyl reductase [62]. Per definition, compounds Mg-PME and Pchlide contain an 8-ethyl substituent. In the present investigation, Pchlide is used as a broader term that also comprises 8-vinyl Pchlide.

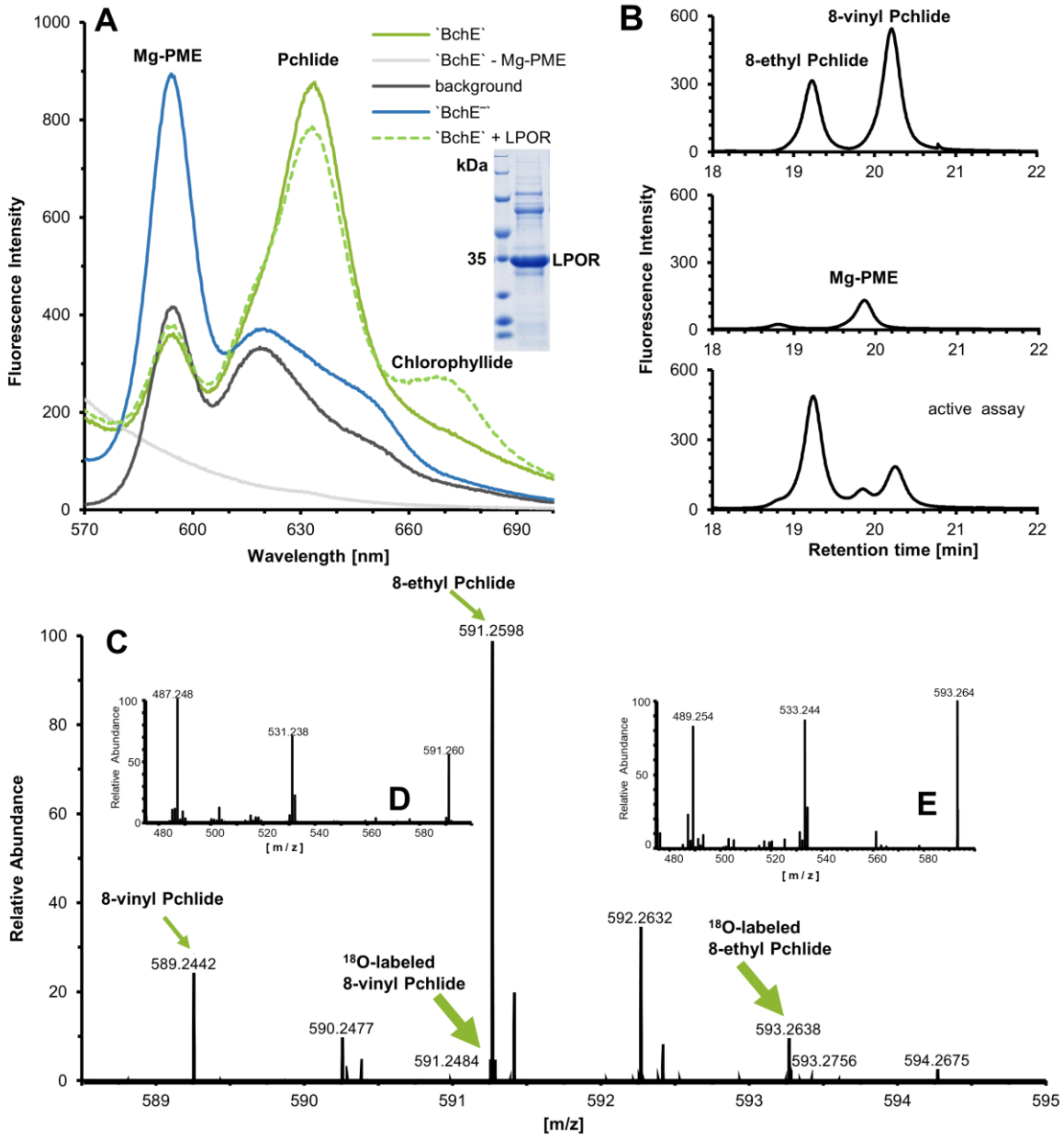

Figure 2. I*n vitro* BchE assay and reaction product characterization by HPLC and $H_2{}^{18}O$ isotope label transfer.
(**A**) BchE activity assay (*green line*, `BchE`) using a cell-free extract of the *bchH*¯ strain (with a blockage of the overall BChl *a* biosynthetic pathway) supplemented with the substrate Mg-PME (140 µM) in the presence of NADPH (2 mM), SAM (2 mM) and 1 mM DTT. Pchlide formation was analyzed by fluorescence spectroscopy (λ_{ex} = 438 nm, λ_{em} = 633 nm). A control reaction in the absence of Mg-PME (*grey line*, `BchE`- Mg-PME) and the signal of the purified Mg-PME in assay buffer (*black*, background; λ_{em} = 595 nm) is shown. Control reaction using a BchE-depleted cell-free extract of the *R. capsulatus bchE*¯ strain (*blue line*, `BchE¯`) instead of the extract from strain *bchH*¯. BchE-dependent conversion of Mg-PME into chlorophyllide using LPOR (*green dashed line*, `BchE`+ LPOR). The *in vitro* assay was supplemented with 3.3 µM heterologously overproduced and purified LPOR (*inlet*), 2 mM NADPH followed by light incubation. Conversion of Mg-PME into Pchlide and subsequent chlorophyllide formation (λ_{em} = 670 nm) is demonstrated (*bottom*). (**B**) HPLC analysis of BchE reaction products (fluorescence detection, λ_{ex} = 438 nm; λ_{em} = 633 nm). A mixture of Pchlide and 8-vinyl Pchlide (19.2 and 20.3 min, *top*) and a purified Mg-PME sample (19.8 min, *middle*) were used as a reference. The *in vitro* activity assay revealed parallel formation of Pchlide and 8-vinyl Pchlide (*bottom*). (**C**-**E**) Positive ion electrospray mass spectrum of partially ^{18}O labeled BchE reaction products 8-ethyl Pchlide and 8-vinyl Pchlide (*green arrows*, unlabeled; *green bold arrows*, mono-^{18}O-labeled). An *in vitro* activity assay was performed in the presence of ~ 20% (v/v) $H_2{}^{18}O$. Derivatives were unequivocally identified by their exact masses: found m/z 591.2598, calculated 591.2602 for $C_{35}H_{35}N_4O_5^+$ and found m/z 593.2638, calculated 593.2644 for the mono-^{18}O-labeled derivative of 8-ethyl Pchlide. Similar fragmentation behaviour of unlabeled and labeled 8-ethyl Pchlide (loss of acetic acid followed by CO_2) upon collision induced dissociation is shown in the MS/MS spectra D and E. The weaker signals at m/z 589.2442 and 591.2484 correspond to 8-vinyl Pchlide and the related ^{18}O-labeled derivative (both with a vinyl group instead of ethyl on C8). (**A**-**E**) All enzymatic experiments were performed under strict anoxic conditions.

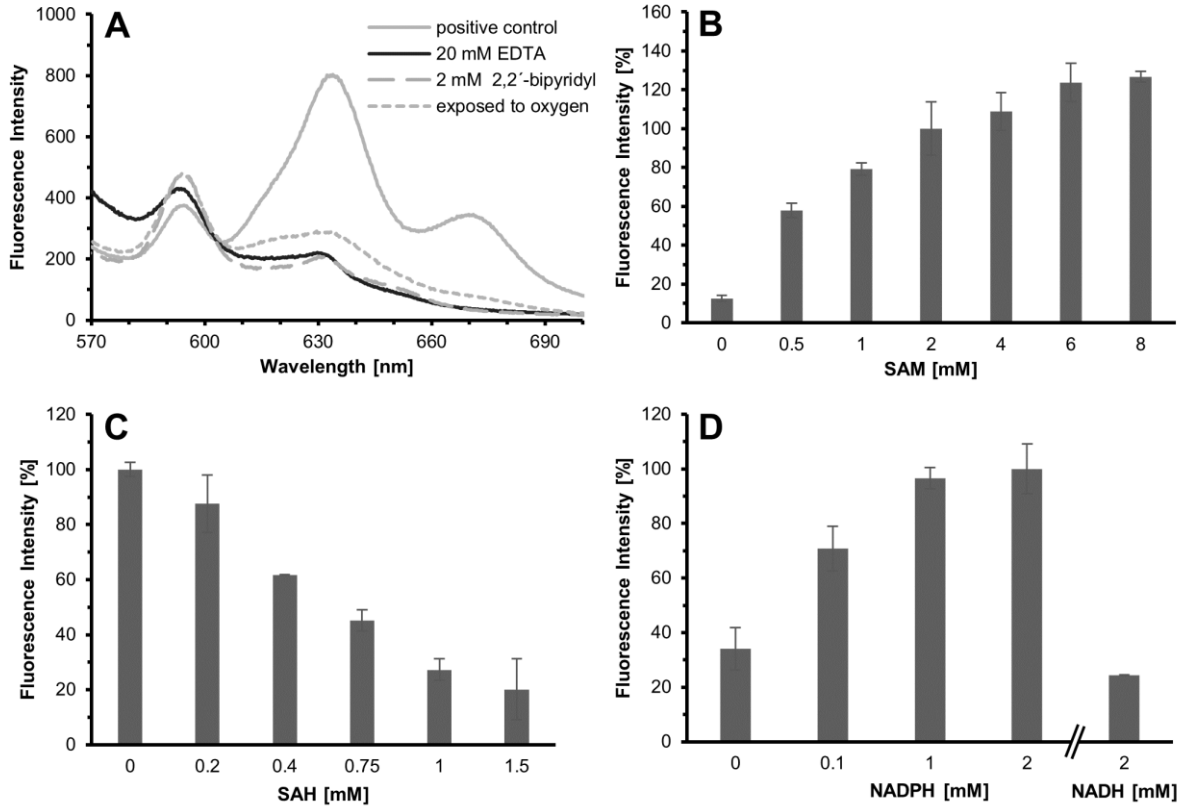

Figure 3. Cofactor requirements and inhibition of BchE catalysis.
(**A**) The *in vitro* activity assay (*positive* control) was used to study the inactivation of BchE using chelators EDTA (20 mM) and 2,2′-Bipyridyl (2 mM) or in the presence of molecular oxygen (air exposure for 10 min). (**B**) and (**D**) BchE activity is stimulated by increasing concentrations of SAM and NADPH. (**C**) BchE inhibition with increasing concentrations of the cofactor analog S-adenosylhomocysteine (SAH) in the presence of 2 mM SAM. If not indicated otherwise, assays contained Mg-PME (0.14 mM), SAM (2 mM), NADPH (2 mM) and DTT (1 mM) and were performed under strict anoxic conditions.

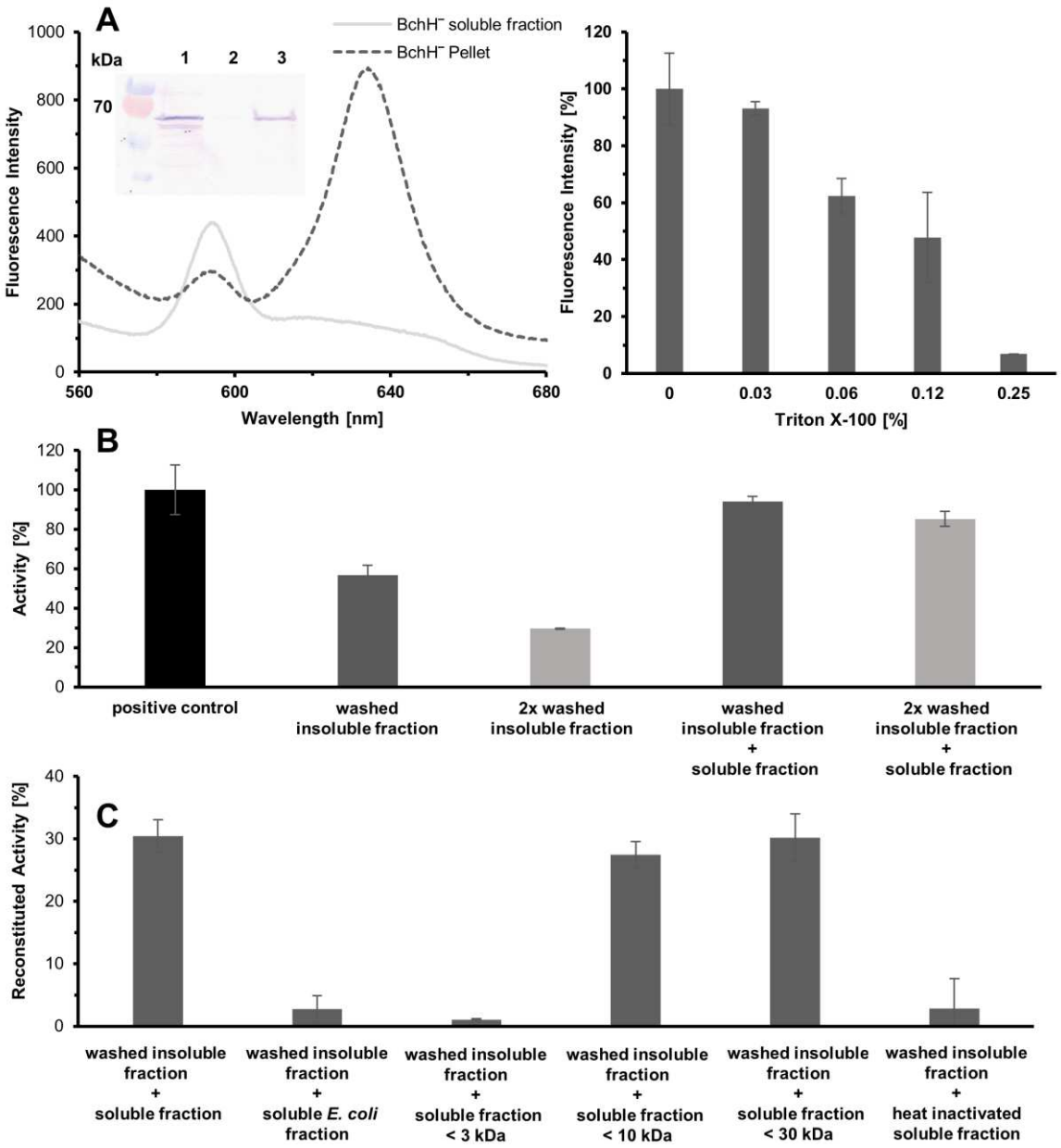

Figure 4. Reconstitution of BchE activity using insoluble and soluble protein fractions.

(**A**) Subcellular fractionation of wild-type *R. capsulatus* cells analyzed by BchE antibodies (*inlet left panel*): cell-free extract (*lane* 1), soluble supernatant after ultracentrifugation (*lane* 2) and insoluble fraction (*lane* 3). The *in vitro* activity assay indicates the localization of BchE: assay using a soluble (*grey*) or an insoluble (*dotted black*) fraction of the *bchH*⁻ strain (after a single centrifugation step) solely revealed activity for the insoluble fraction. The *in vitro* activity assay is inhibited by increasing concentrations of Triton X-100 (*right panel*) (**B**) Reconstitution of BchE activity using insoluble and soluble fractions. One or two additional washing steps for the insoluble fraction revealed a clear decrease of the BchE activity (*washed insoluble fraction* or *2x washed insoluble fraction*). In both cases, BchE activity was restored when the insoluble fraction was combined with the soluble fraction (*washed insoluble fraction + soluble fraction* or *2x washed insoluble fraction + soluble fraction*). (**C**) Identical reconstitution experiments using a soluble extract from wild-type *E. coli* cells did not restore BchE activity (*washed insoluble fraction + soluble E. coli fraction*). The soluble *R. capsulatus* extract (from B) was size fractionated by ultrafiltration using membranes with a 3, 10 and 30 kDa cut-off, respectively. Only the <30 kDa and the <10 kDa filtrate was able to restore BchE activity (*washed insoluble fraction + soluble fraction < 30 kDa* and *washed insoluble fraction + soluble fraction < 10 kDa*). The < 3 kDa filtrate (*washed insoluble fraction + soluble fraction < 3 kDa*) and a heat inactivated soluble fraction (*washed insoluble fraction + heat inactivated soluble fraction*) did not support BchE activity.

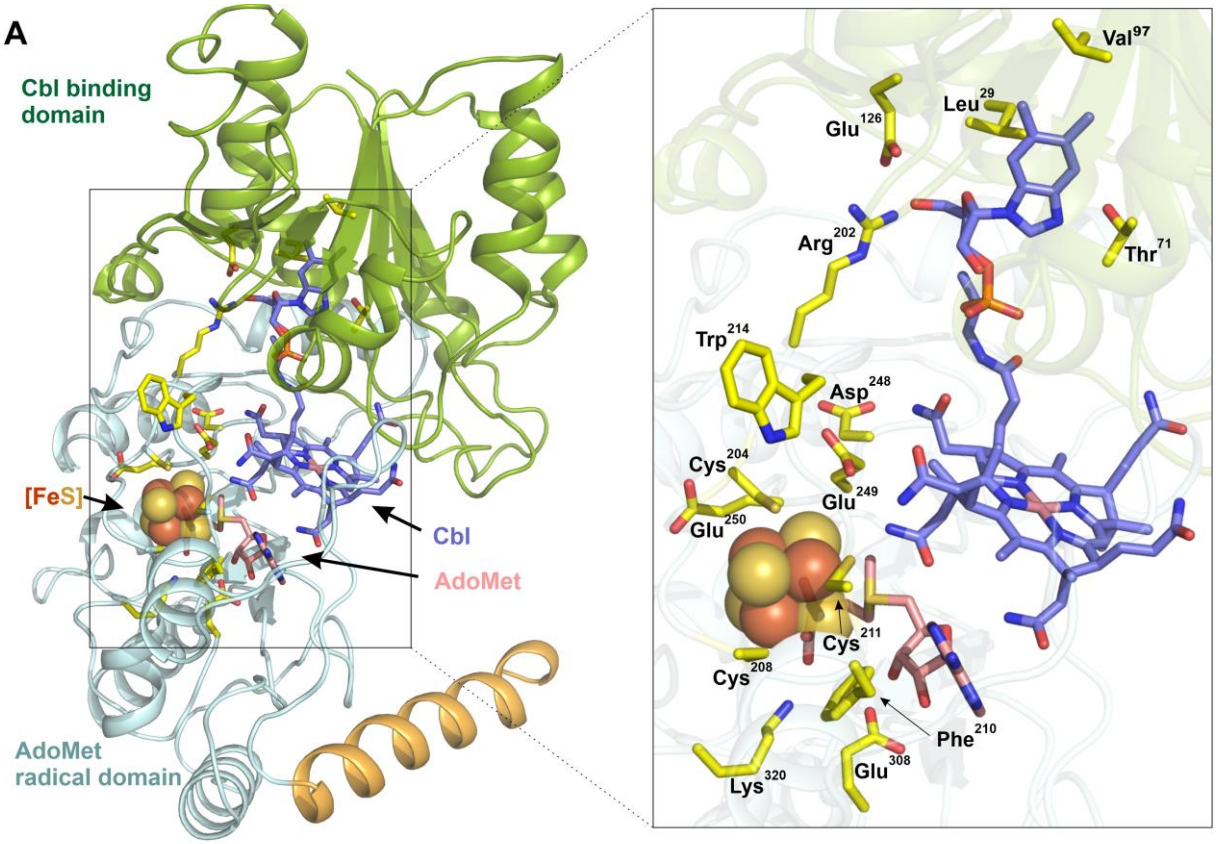

Figure 5. Structural modelling of BchE and partial sequence alignment.

(**A**) A homology model (comprising amino acid residues 1–433, *left*) based on the structure of OxsB (PDB code: 5UL3) was calculated using SWISS-MODEL [29]. Superposition of the tentative BchE structure with 5UL3 (with a bound cobalamin cofactor) revealed an N-terminal cobalamin (Cbl) binding domain (residues 1-196, *green*), the adenosylmethionine (AdoMet) radical domain (residues 197-412, *light blue*) containing a [4Fe-4S] cluster (*spheres*) and adenosylmethionine (AdoMet, *pale pink*) followed by a C-terminal helix (*orange*). Highly conserved BchE residues were identified (*yellow sticks*) and subsequently explored in a structure guided mutagenesis approach. Exchanged amino acid residues are highlighted in a close up representation (*right*). The figure was created with PyMOL [30]. (**B**) Partial alignment of representative BchE sequences from *R. capsulatus* (residues in single-letter code), *Rhodobacter sphaeroides*, *Dinoroseobacter shibae*, *Synechocystis* PCC 6714, *Chlorobaculum tepidum* and *Rubrivivax gelatinosus*.

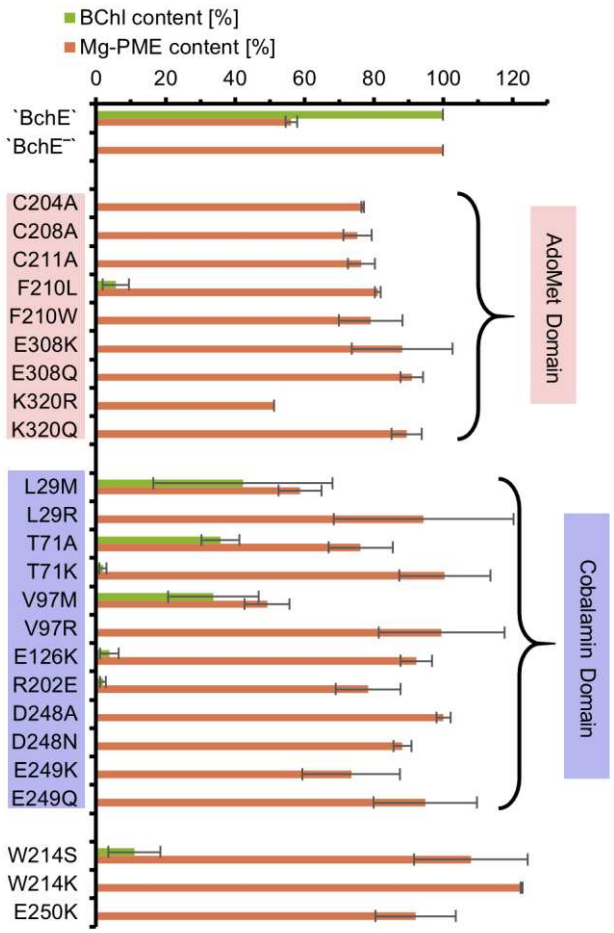

Figure 6. Enzymatic activity of variant BchE proteins.
An *in vivo* complementation assay was performed using the complemented *R. capsulatus bchE¯* strain. Plasmids were transferred into the *bchE¯* strain by diparental mating and the presence of complementing *bchE* gene was verified by PCR. Strains were cultivated under microaerophilic conditions and the presence of identical amounts of BchE was verified by western blot analyses. The amount of BChl *a* or of Mg-PME was determined spectroscopically (absorption at 772 nm or 415 nm) using organic extraction procedures, respectively. Green columns: BChl *a* content in % compared to the complemented strain *R. capsulatus bchE¯*/pRhoKs_Gm_*bchE* (BChl *a* content set as 100%, `*BchE*`). Pale orange columns: Mg-PME content in % compared to strain *R. capsulatus bchE¯*/pRhoKs_Gm (Mg-PME content set as 100%, ´*BchE¯*´).